Fig. S1. Design and TLR ligand response of mouse and human macrophage reporter cell lines for siRNA screening applications. (**A**) Design of the dual-promoter lentiviral vector for the expression of NF-κB and TNF-α reporters in the mouse RAW264.7 cell line–derived RAW G9 clone. Gene cassette 1 contains the mouse *Tnf* promoter driving expression of an mCherry-PEST fusion protein, and gene cassette 2 contains the mouse *Rela* promoter driving expression of a GFP-relA fusion protein. (**B** and **C**) *Tnf* promoter-driven mCherry expression at 16 hours (B) and the cytosol-to-nuclear translocation of the GFP-RelA fusion at 40 min (C) in RAW G9 cells after treatment with LPS (10 ng/ml), 100 nM P3C, or R848 (10 μg/ml). (**D**) Design of the dual-promoter lentiviral vector for expression of the TNF-α reporter in the human THP1 cell line–derived THP1 B5 clone. Gene cassette 1 contains the human *TNF* promoter driving TLR ligand-inducible expression of firefly luciferase, and gene cassette 2 contains the human *UBC* promoter driving constitutive expression of renilla luciferase. (**E**) The firefly:renilla luciferase expression ratio in THP1 B5 cells at 4 hours after treatment with LPS (10 ng/ml). Data in (B), (C), and (E) are means ± SD of three experiments. **$P < 0.01$, ***$P < 0.001$, ****$P < 0.0001$ by two-tailed t test.

Toll-like receptors

Proximal MyD88 signaling

NFkB module

MAPK module

TRIF module

PI3K-Akt signaling

Transcription factors

Cytokines

Negative regulators
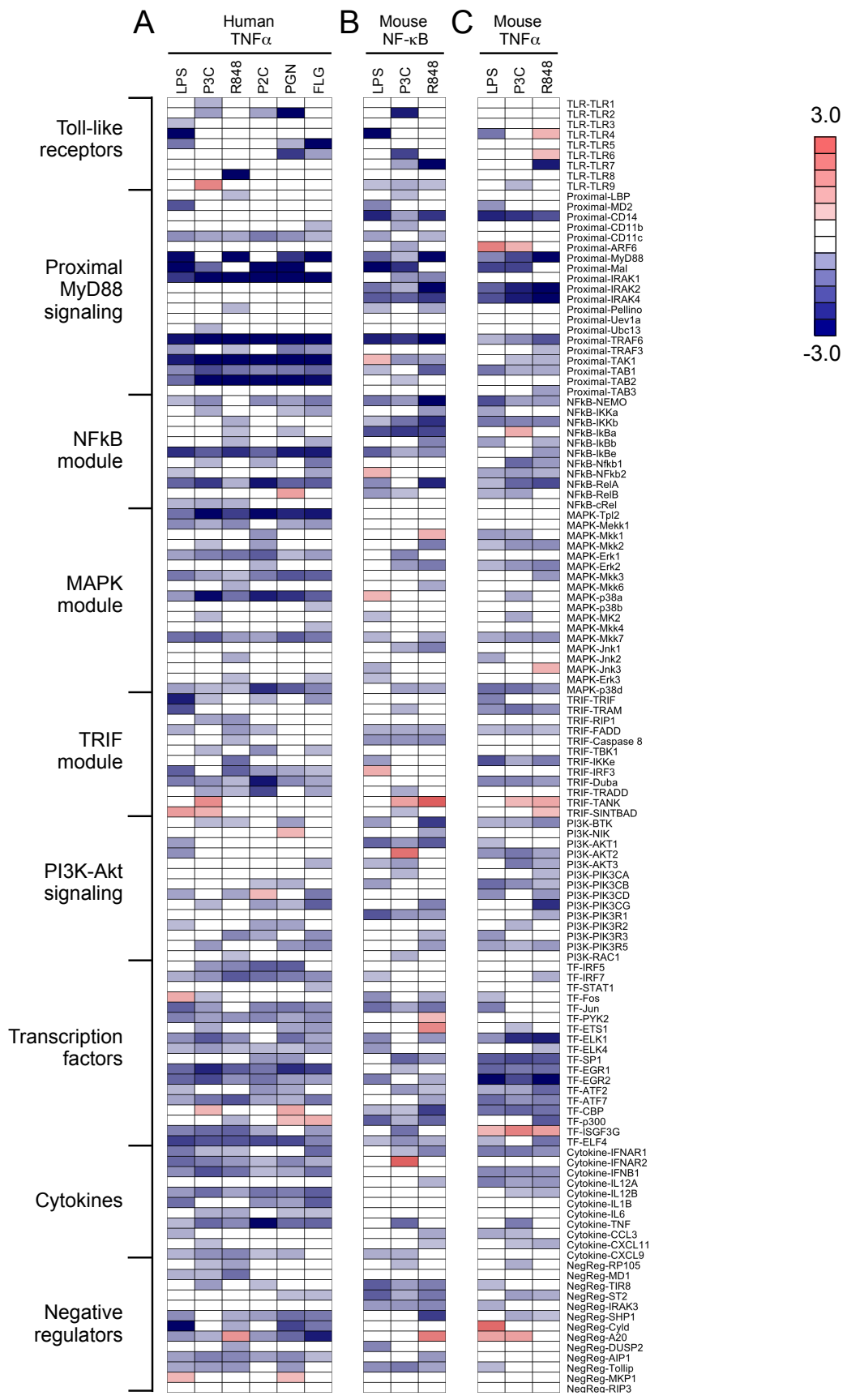
Fig. S2. Effects of siRNA-mediated gene perturbations across the human and mouse TLR pathways. (**A** to **C**) TLR pathway gene perturbation effects on (A) the *TNF* promoter–driven transcriptional response of human THP1 cells to LPS (10 ng/ml), 100 nM P3C, R848 (10 μg/ml), 1 nM P2C, PGN (10 μg/ml), or FLG (10 ng/ml) and (B) the NF-κB–driven and (C) the *Tnf* promoter–driven responses of mouse RAW264.7 cells to LPS (10 ng/ml), 100 nM P3C, or R848 (10 μg/ml). Data are equivalent to those shown in Fig. 2, A and D, but are enlarged to include TLR pathway modules and gene names. Data are presented as median z-scores from six siRNAs per gene. Individual siRNA z-scores were averaged from three (A) or two (B and C) independent experiments (see Materials and Methods for details).

Human TNFα · Mouse TNFα

LPS P3C R848 LPS P3C R848

TLR-TLR9
TLR-TLR6
MAPK-Jnk3
TRIF-TANK
TRIF-SINTBAD
NegReg-MKP1
TLR-TLR1
TLR-TLR2
Proximal-Ubc13
TRIF-TBK1
MAPK-MK2
TF-ETS1
TF-Fos
NFkB-IKKa
NegReg-TIR8
PI3K-PIK3CG
TLR-TLR7
Proximal-TAB3
PI3K-PIK3CA
PI3K-PIK3R1
TF-p300
PI3K-BTK
MAPK-Mkk2
PI3K-PIK3R5
NFkB-NEMO
NFkB-RelA
TF-ELK1
TF-EGR2
TRIF-Duba
MAPK-p38d
Cytokine-IFNAR1
TF-ATF7
MAPK-Mkk7
Proximal-TAB1
TF-EGR1
Cytokine-IFNB1
TRIF-TRAM
NFkB-NFkb2
PI3K-AKT2
TF-ATF2
Proximal-IRAK4
Proximal-IRAK2
MAPK-Erk2
TF-CBP
PI3K-PIK3CB
Proximal-CD14
TF-SP1
Cytokine-IL12A
NFkB-Nfkb1
Cytokine-CXCL11
PI3K-AKT3
NegReg-ST2
NFkB-IkBb
NFkB-IKKb
TRIF-IKKe
PI3K-PIK3CD
MAPK-Jnk2
PI3K-PIK3R3
NFkB-RelB
MAPK-Mkk1
NegReg-IRAK3
Proximal-MD2
PI3K-AKT1
TRIF-TRIF
TF-Jun
TLR-TLR4
TLR-TLR3
TLR-TLR5
Cytokine-IL1B
PI3K-PIK3R2
Proximal-Mal
Cytokine-CCL3
Proximal-TRAF3
TRIF-IRF3
Proximal-MyD88
TRIF-FADD
NegReg-SHP1
NegReg-Cyld
NFkB-IkBa
TF-ISGF3G
TLR-TLR8
Proximal-LBP
Proximal-Pellino
MAPK-Mkk6
MAPK-Erk3
TRIF-Caspase 8
PI3K-RAC1
NegReg-DUSP2
TRIF-TRADD
TRIF-RIP1
TF-IRF5
Cytokine-IL6
NegReg-RP105
Proximal-TRAF6
Cytokine-IL12B
MAPK-p38a
Cytokine-TNF
TF-IRF7
MAPK-Mkk3
TF-ELK4
NFkB-IkBe
TF-ELF4
NegReg-MD1
MAPK-Mekk1
Proximal-CD11c
TF-PYK2
Cytokine-IFNAR2
Proximal-TAK1
MAPK-Tpl2
Proximal-IRAK1
Proximal-TAB2
MAPK-Erk1
Cytokine-CXCL9
NFkB-cRel
NegReg-AIP1
NegReg-Tollip
Proximal-CD11b
Proximal-Uev1a
MAPK-p38b
MAPK-Mkk4
MAPK-Jnk1
PI3K-NIK
TF-STAT1
Proximal-ARF6
NegReg-A20
NegReg-RIP3

3.0

-3.0

Fig. S3. Human and mouse macrophages show both shared and distinct gene dependencies in TLR signaling. Hierarchical clustering analysis (Pearson uncentered, average linkage) of the human and mouse macrophage *TNF/Tnf* promoter–driven responses to LPS, P3C, and R848. Data are equivalent to those shown in Fig. 3A, but are enlarged to include TLR pathway modules with gene names. Data are presented as median z-scores from six siRNAs per gene. Individual siRNA z-scores were averaged from three (human TNF-α readout) or two (mouse TNF-α readout) independent experiments (see Materials and Methods for details).
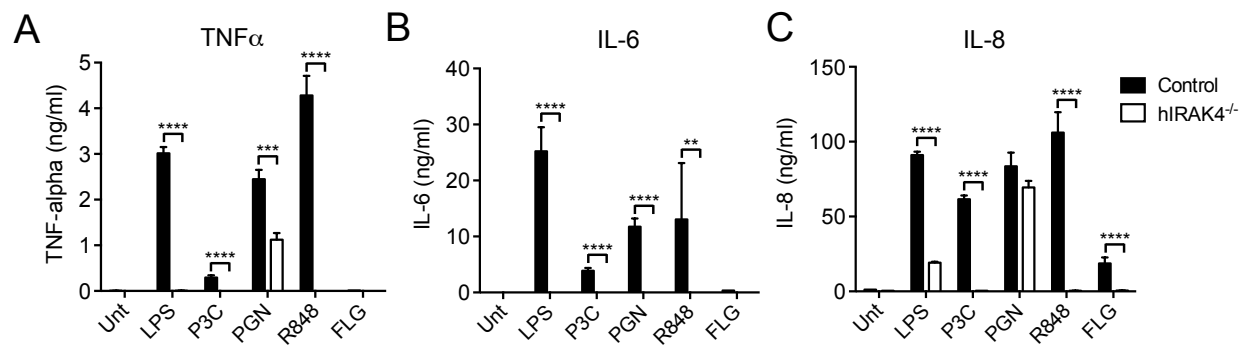
Fig. S4. IRAK4 is required for the responses of human PBMCs to TLR ligands. (**A** to **C**) Human PBMCs isolated from control and IRAK4-deficient human patients were stimulated for 24 hours with LPS (10 ng/ml), 100 nM P3C, PGN (10 μg/ml), R848 (10 μg/ml), or FLG (10 ng/ml) before the secreted amounts of the indicated cytokines were measured by Bioplex assay. Data are means ± SD of two independent biological replicates from one set of patient blood samples. **$P < 0.01$, ***$P < 0.001$, ****$P < 0.0001$ by two-tailed t test.
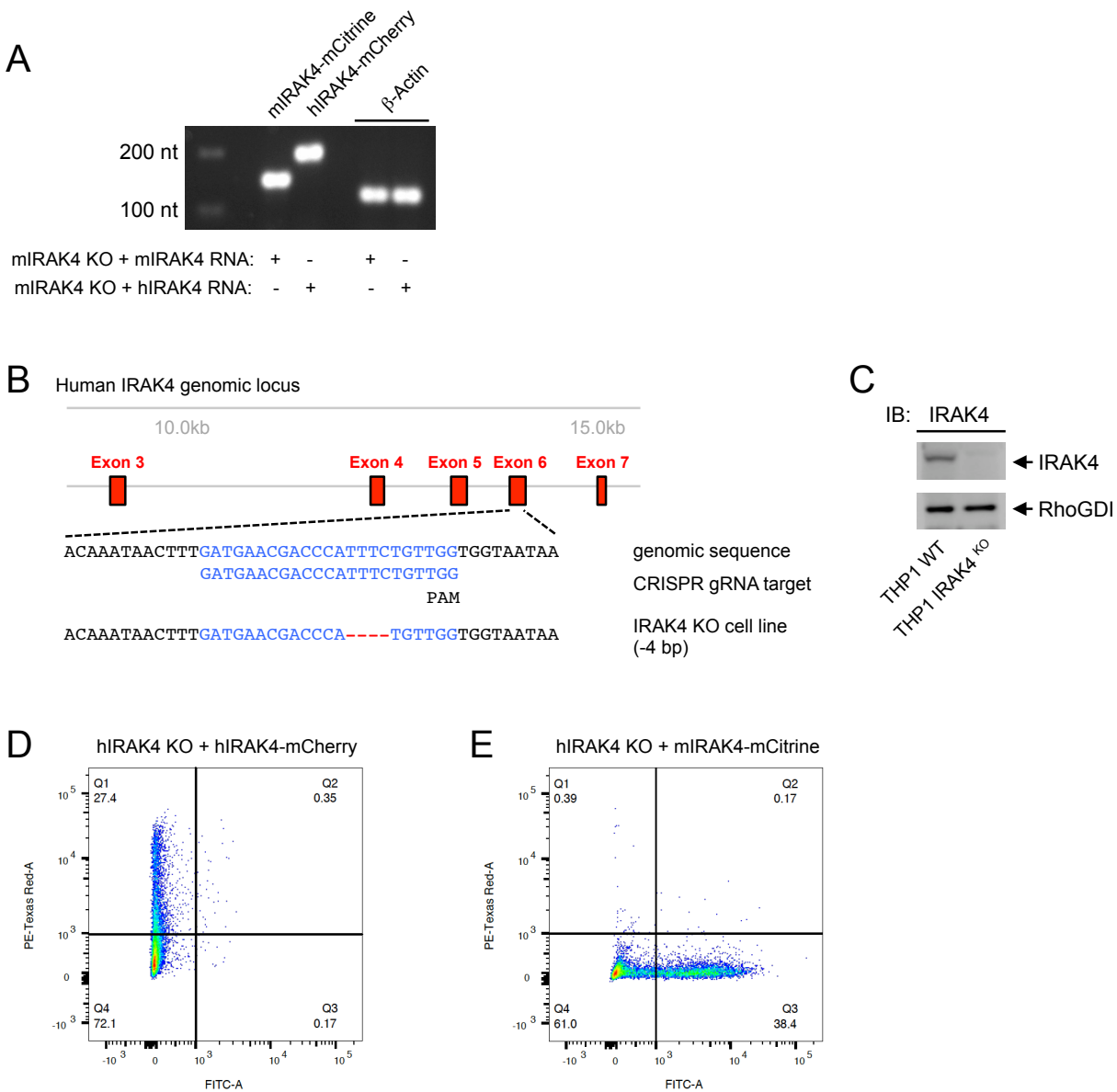
Fig. S5. Generation of IRAK4 rescue cell lines from IRAK4 KO IMMs and THP1 cells. (**A**) The relative abundances of the re-expressed mouse and human IRAK4 fluorescent protein fusions in IRAK4-deficient mouse IMMs were measured by RT-PCR assays. The amounts of β-actin mRNA in each cell line are shown as RNA input controls. (**B**) Schematic showing the exons targeted for CRISPR/Cas9-mediated genome editing of the human *IRAK4* gene locus in THP1 cells. The guide RNA (gRNA) target sequence is shown with the 3' NGG PAM sequence, and the resulting genome edit within the gRNA for the IRAK4 KO cell clone is indicated. (**C**) Western blotting analysis of WT THP1 cells and the THP1 IRAK4 KO cell line was performed with antibody against IRAK4. (**D** and **E**) The relative abundances of the human IRAK4-mCherry (D, Texas Red channel) and the mouse IRAK4-mCitrine (E, FITC channel) fusion proteins re-expressed in the IRAK4-deficient human THP1 cell line were measured by flow cytometry. Data in (A) and (C) to (E) are representative of two independent experiments.
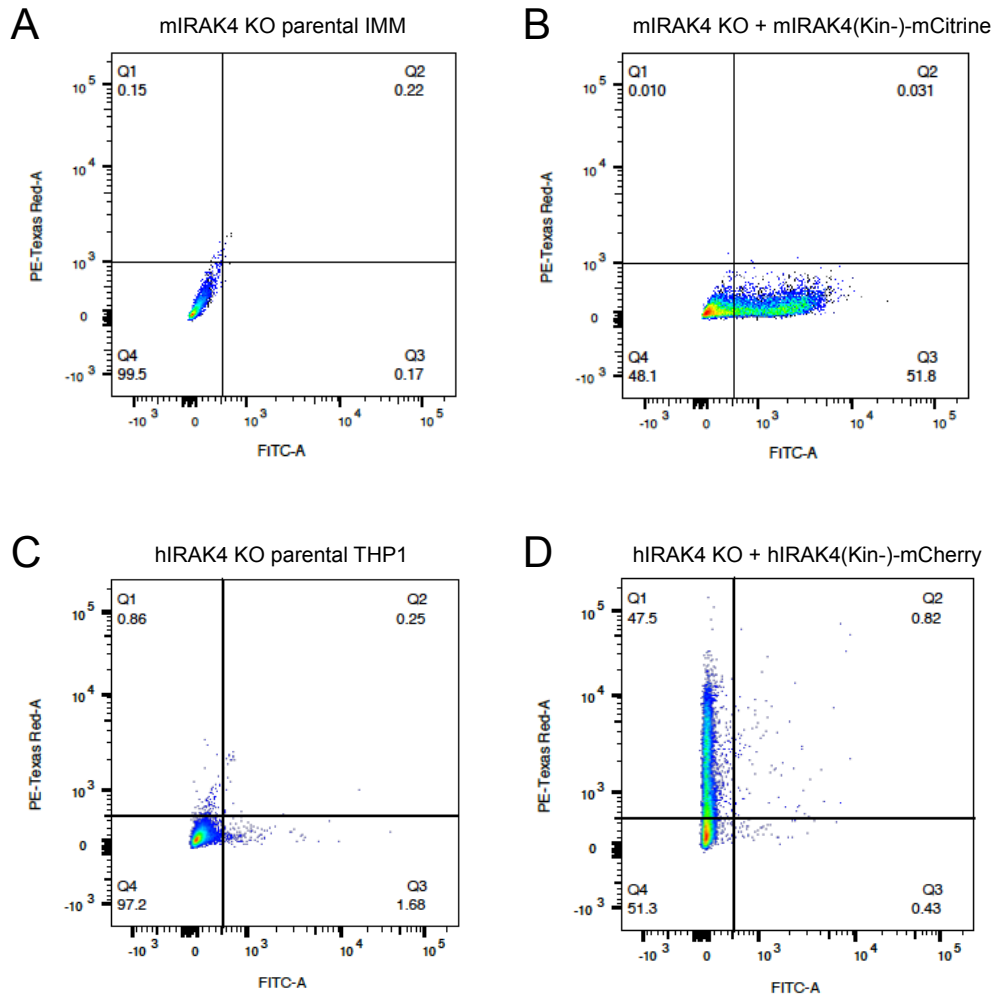
Fig. S6. Expression of kinase-deficient mouse and human IRAK4 in IRAK4 KO mouse IMMs and THP1 cells. (**A** and **B**) Flow cytometric analysis of the amount of the mouse IRAK4-mCitrine kinase-deficient mutant in retrovirally transduced IRAK4 KO IMMs (B, FITC channel) relative to that in parental IRAK4 KO IMMs (A). (**C** and **D**) Flow cytometric analysis of the amount of the human IRAK4-mCherry kinase-deficient mutant in retrovirally transduced IRAK4 KO THP1 cells (D, Texas Red channel) relative to that in the parental IRAK4 KO THP1 cell line (C). Data are representative of two independent measurements of cells at different passage numbers.
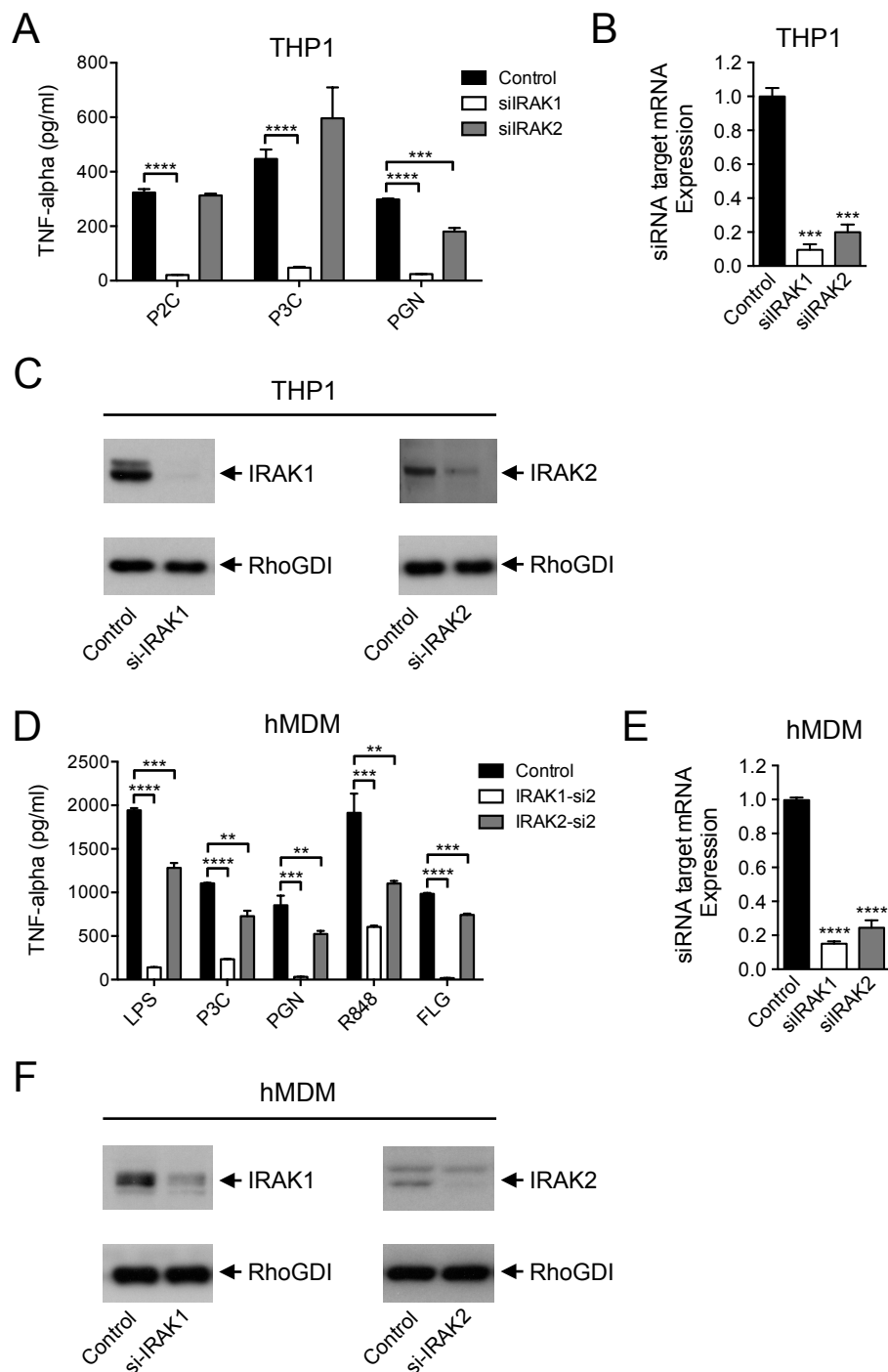
Fig. S7. Analysis of the IRAK1-dependency of human macrophages for TLR responses. (**A**) THP1 cells transfected with control, IRAK1-specific, or IRAK2-specific siRNA were stimulated with 10 nM P2C, 100 nM P3C, or PGN (10 μg/ml) for 24 hours before the amounts of secreted TNF-α were measured. (**B** and **C**) THP1 B5 reporter cells transfected with control, IRAK1-specific, or IRAK2-specific siRNA were analyzed by qRT-PCR (B) and Western blotting assays (C) to determine the efficiency of target knockdown. Mean protein abundances in knockdown cells relative to those in control cells calculated from combined experiments were as follows: IRAK1: 0.12 ± 0.02 (*P* < 0.0001); IRAK2: 0.20 ± 0.02 (*P* < 0.0001). Statistical analysis was by

two-tailed t test. (**D**) hMDMs transfected with control, IRAK1-specific, or IRAK2-specific siRNA (different siRNAs from those shown in Fig. 5D) were stimulated for 24 hours with LPS (10 ng/ml), 100 nM P3C, PGN (10 μg/ml), R848 (10 μg/ml), or FLG (10 ng/ml) before the amounts of secreted TNF-α were measured by ELISA. (**E** and **F**) hMDMs transfected with control, IRAK1-specific, or IRAK2-specific siRNA were analyzed by qRT-PCR (E) and Western blotting assays (F) to determine the efficiency of target knockdown. Mean protein abundances in knockdown cells relative to those in control cells calculated from combined experiments were as follows: IRAK1: 0.44 ± 0.06 ($P < 0.01$); IRAK2: 0.26 ± 0.05 ($P < 0.001$). Statistical analysis was by two-tailed t test. Data in bar graphs are means $\pm$ SD of three experiments. Western blots are representative of three independent experiments. **$P < 0.01$, *** < 0.001, ****$P < 0.0001$ by two-tailed t test.
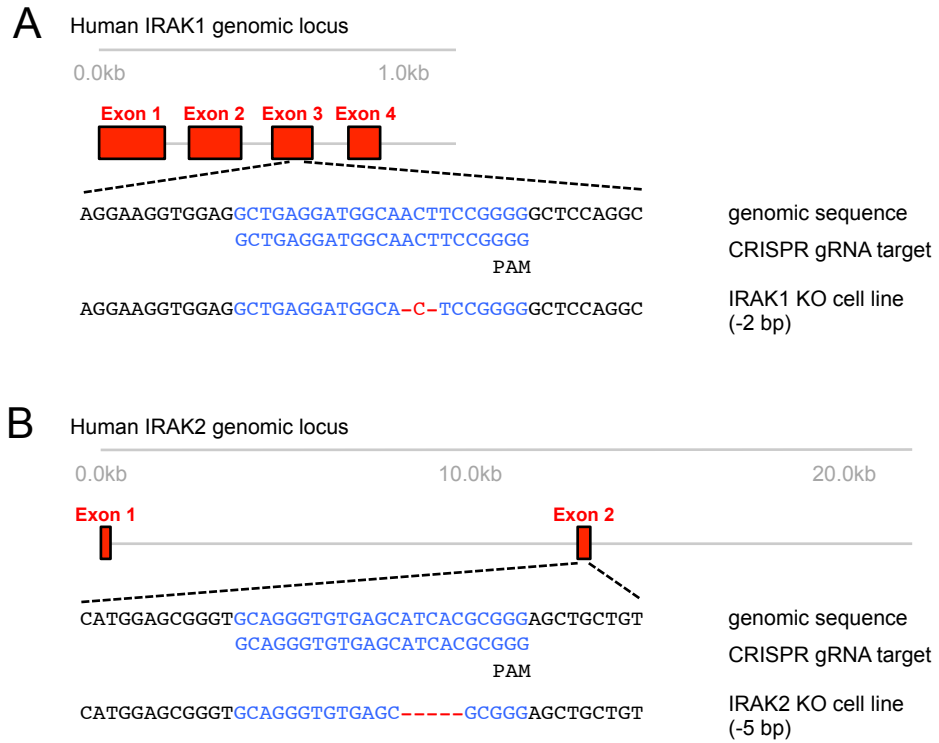
Fig S8. CRISPR/Cas9-mediated targeting of the human *IRAK1* and *IRAK2* loci in THP1 cells. (**A** and **B**) Schematics indicate the exons targeted for genome editing at the (A) *IRAK1* and (B) *IRAK2* human gene loci. In each case, the guide RNA (gRNA) target sequence is shown with the 3' NGG PAM sequence, and the resulting genome edit within the gRNA for each IRAK KO cell clone is indicated.
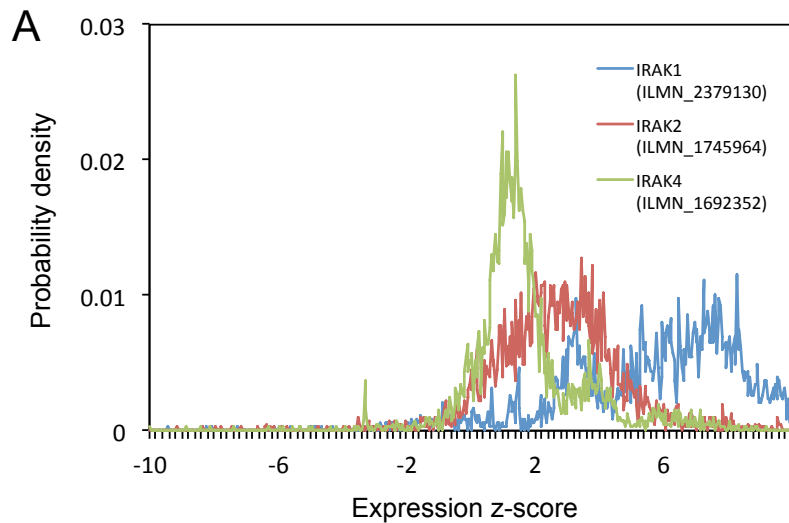
GeneSymbol	EntrezID	Probe.Set.ID	Min	Max	Median	SD	MAD
IRAK1	3654	ILMN_2379130	-9.41	10.00	6.15	2.74	2.63
IRAK2	3656	ILMN_1745964	-9.14	9.99	2.67	1.96	1.67
IRAK4	51135	ILMN_1692352	-9.99	9.22	1.41	1.77	0.93
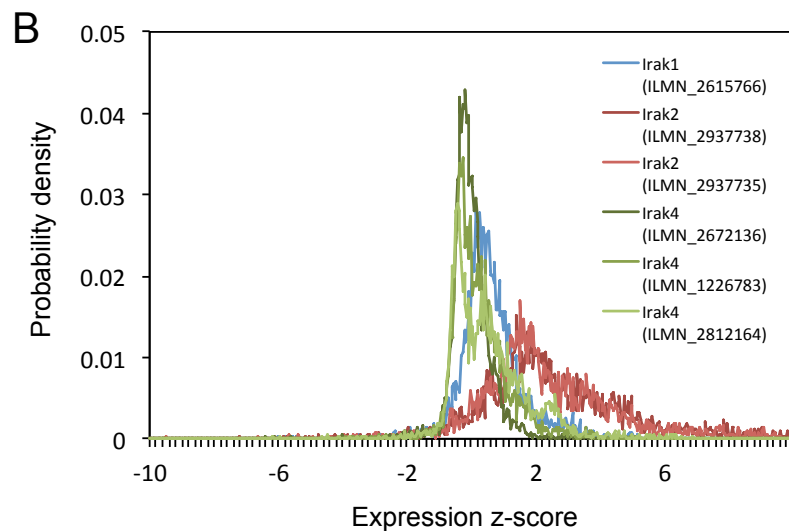
GeneSymbol	EntrezID	Probe.Set.ID	Min	Max	Median	SD	MAD
Irak1	16179	ILMN_2615766	-6.02	5.70	0.49	0.99	0.68
Irak2	108960	ILMN_2937738	-7.22	9.82	2.18	2.17	1.80
Irak2	108960	ILMN_2937735	-9.50	9.93	1.95	2.06	1.60
Irak4	266632	ILMN_2672136	-6.37	5.13	-0.09	0.62	0.42
Irak4	266632	ILMN_1226783	-3.92	5.64	0.08	0.87	0.66
Irak4	266632	ILMN_2812164	-6.17	6.89	0.30	1.17	1.01

Fig. S9. Expression distributions of IRAK1, IRAK2, and IRAK4 mRNAs in human and mouse GEO datasets. (**A** and **B**) Probability distributions of the expression z-scores for (A) human *IRAK1*, *IRAK2*, and *IRAK4* and (B) mouse *Irak1*, *Irak2*, and *Irak4* calculated from all available normalized gene expression data for platforms GPL6884 (Illumina HumanWG-6 v3.0 expression beadchip) and GPL6885 (Illumina MouseRef-8 v2.0 expression beadchip). See Materials and Methods for details about the z-score calculation. Tables below the graphs show minimum, maximum, median, standard deviation, and median absolute deviation of the distributions for each IRAK gene probe. If multiple probes were available for the same gene, they are shown separately.

Table S1. Details of the siRNAs used to target the 126 human and mouse TLR pathway genes. File includes gene symbols and gene IDs with corresponding siRNA plate locations, vendor ID, and sequence information. Separate spreadsheets are included for the human and mouse siRNAs.

Table S2. siRNA z-scores from screens of the 126 human and mouse TLR pathway genes. File includes gene symbols and gene IDs with both median and individual siRNA scores for each TLR ligand and readout tested. Separate spreadsheets are included for the human and mouse screens. Individual siRNA scores are means from replicate screening experiments (see Materials and Methods for details).

Table S3. Ranking scores of human and mouse TLR pathway genes from the siRNA screens. For each TLR ligand and readout tested, the 126 TLR pathway genes were sorted by their median z-score and assigned ranks from 1 (lowest score) to 126 (highest score) for each ligand-readout combination. For each readout (human TNF-α, mouse NF-κB, and mouse TNF-α), the gene ranks were summed across all ligands tested to obtained the "Species-rank-'readout'-SUM" value. Genes were sorted by these SUM values to obtain ranks from 1 to 126 representing the greatest-to-least perturbation of signal across the TLR ligands for each of the human TNF-α, mouse NF-κB, and mouse TNF-α readouts.

Table S4. Human vs. mouse z-score differences across matched TLR ligands and assay readouts. File includes gene symbols and gene IDs with median siRNA scores for the LPS, P3C, and R848 ligands tested with both the human and mouse TNF-α assay readouts. The average z-score difference between human and mouse shows lower values (green) for genes with stronger effects on the human TLR pathways and higher values (red) for genes with stronger effects on the mouse TLR pathways.